Egyptian Journal of Chemistry

http://ejchem.journals.ekb.eg/

New Synthesis of BaO nanoparticles Using the UV-Irradiation Technique for Removal Cibacron Blue Dye from their Aqueous Solution

Ahmed Radhi Laftah[1], Ahmad Hussain Ismail [1], Ahmed Mahdi Rheima[1*], Amel Muhson Naji [2]

[1]Department of Chemistry, College of Science, Mustansiriyah University, Baghdad, Iraq.
[2] Department of Optics Techniques, Dijlah University College, Al-Masafi Street, Al-Dora, Baghdad 00964, Iraq

Abstract

This study describes a straightforward and affordable photolysis approach for the large-scale production of barium oxide nanoparticles (BaO-NPs). BaO-NPs were synthesized Using the UV-Irradiation Technique**.** The structural, morphological, compositional, and optical characteristics were studied by XRD, SEM, EDX and PL. the The BaO-NPs crystallite size was determined to be 14.6 nm. the morphology of BaO nanoparticles which demonstrated the existence of nanoparticles in the produced materials. and predicted bandgap of the nanoparticles was determined to be 3.26 eV by photoluminescence spectroscopy. BaO NPS that have been produced exhibit desirable adsorbent behavior for cibacron blue dye in their aqueous solutions. the effects of contact time, adsorbent mass, temperature, and starting cibacron blue dye concentration were investigated. The dye isotherm adsorption demonstrated good Freundlich agreement. The ΔH, ΔS, and ΔG parameters were calculated using a thermodynamic Van't Hoff equation, and the results were 9.69701 kJ/mol, 0.813 kJ/mol K, and 9.403 kJ/mol, respectively. Additionally, the kinetic investigation revealed that the adsorption exhibited pseudo-second-order behavior.
Keywords: UV-Irradiation, Photolysis, BaO NPs, photoluminescence

1. **Introduction**

The vast applications of nanoscience and nanotechnology, which depend on their structure and scale, give them a prominent role in scientific research[1]. Nanoparticles are useful in many different fields because of their unique physical, chemical, electrical, mechanical, medical, biological, catalytic, optical, and magnetic capabilities[2]. Precipitation, sonochemical[3], solid state, sol-gel[4], microwave[5], hydrothermal[6], supersaturated reverse micelles, and microemulsion method are only a few of the many techniques used to create nanoparticles[7]. Metal oxides have a special role in the evolution of nanospecies because of the diverse range of characteristics that allow them to be used in so many different contexts[8]. Semiconductor nanoparticles, in particular, have promising uses in catalysis, sensors, photoelectron, highly functional, and efficient devices[9]. Among different metal Due to its broad bandgap[10], barium oxide in particular occupies a special position[11]. The standard of water throughout Rapid industrialization directly affects the planet and the rapid expansion of the population. A nation's development depends on its industrial expansion[12]. As various sectors reject life-threatening sewage entering aquatic systems, which is not good influences the water's quality[13]. The fabric, printing, papermaking, cosmetics, food processing, and the pharmaceutical industry releases its effluents into thewater bodies with high levels of colors and dyes[14]. It has been discovered to be neurotoxic, chronically toxic, and carcinogenic to both people and animals. Dye treatment from industrial effluents is necessary before they pose a threat to the environment[15] . In addition to harming the beauty of the river, dyes also hinder sunlight's ability to pass through water, which has an impact on how aquatic plants synthesize food. In the present study, BaO NPS adsorption of cibacron blue dye. BaO NPS prepared by photolysis methods and were characterized through SEM, EDX, XRD, PL. and study its kinetic with thermodynamic properties.

*Corresponding author e-mail: ahmed.rheima@gmail.com.; (Ahmed Radhi Laftah1).
Receive Date: 12 March 2022, **Revise Date:** 24 August 2022, **Accept Date:** 29 August 2022, **First Publish Date:** 29 August 2022
DOI: 10.21608/EJCHEM.2022.126902.5651

2. Experimental

2.1. Materials

Barium acetate (CH3COO)2Ba), urea (NH2)2CO, sodium hydroxide (NaOH) and SibaCrohn blue dye with deionized water were used throughout the preparation period.

2.2. Methods

All chemicals used in this study were purchased from sigma Aldrich without any purification. BaO nanoparticles were synthesized by the photolysis method. As shown in fig. (1), a photocell was used to irradiate the source of BaO NPS . Immersed U.V source (125 w) is used with λ=365nm. The cell contains a quartz tube-like jacket for immersion U.V source in the solution barium. Pyrex counting was used as a reactor. An ice bath cools the reactor to avoid rising temperature due to U.V lamp. Accordingly, 100 ml of 0.4 mole urea was Added slowly (drop per second) to 100 ml of 0.2 mole Barium acetate under a magnetic stirrer for 15 min at 25 C° .then, a photocell irradiated the Barium solution for 30min . The white precipitate is formed it is separated and washed several time with D.W . the powder was dried at 120 ˚C for 3h and calcinated at 600 ˚C for 3 h. A white powder of BaO NPs is obtained[16].

2.3 | Adsorption cibacron blue on BaO NPS

Using 100 mg/L Cibacron Blue dye stock solutions made with distilled water, batch adsorption tests were carried out. The Cibacron Blue dye was added to the solution and extra diluted to the proper quantities (5–25 mg/L). In 200 ml glass tubes, 100 ml of dye solution and 0.01 g of BaO NPS were combined to complete the tests. The glass tubes were set on a shaker (HZQ-C) at different temperatures (15, 25, 35, 45, and 55 °C) and shook for 90 minutes. A UV-visible spectrophotometer was used to calculate the dye concentration. Equation 1 was used to quantify the amount of dye that had been adsorbed in the solution. Qe indicates the equilibrium capacity of adsorption (mg/g), and C_o is the initial concentration of the dye Cibacron Blue (mg)[18].

$$Q_e = (C_o - C_e)\, V_{sol} / m \qquad (1)$$

where Q_e represents the equilibrium capacity of adsorption (mg / g), C_o is the initial Cibacron Blue dye concentration (mg / L), C_e is the equilibrium concentration of Cibacron Blue dye (mg / L), V is the volume of the solution (L), and m is the amount of the BaO NPS.

3 . Results and discussion

3.1. Characterization

BaO-NPs as-synthesised were examined for phase and crystallinity using the XRD method and Cu Ka radiations (λ = 1.5406).Figure 2: As-produced BaO nanoparticles' XRD patterns in the 10–80° range. Fig. (2) displays the XRD spectra of BaO-NPs that were created. The observed XRD pattern contains numerous well-defined peaks that are connected to and well-matched with the tetragonal phase of BaO-NPs and are in good agreement with the "JCPDS" card No. 26-0178. These peaks include (200), (223), (211), (102), (375) and (212), among others. The produced nanoparticles are highly crystalline in character, as indicated by sharp and strong peaks. The Debye-Scherrer formula, which can be written as $D = K\lambda/\beta\cos\theta$ (2)

is used to calculate the sample's average crystallite size (D).where β is the full-width at half maximum, K is the form factor (0.90), and is the wavelength of Cu Ka radiation (λ=1.5406).θ The diffraction angle is . BaO-NPs are discovered to have an average grain size of about (14.6nm) [11] .

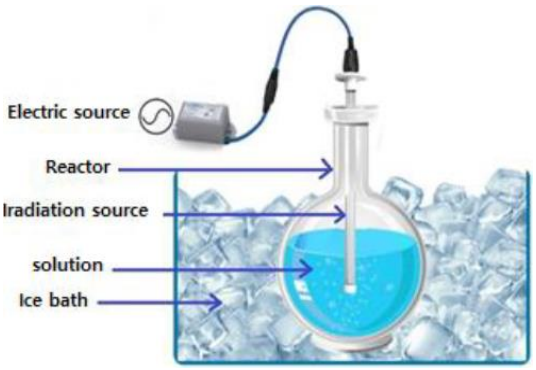

Figure 1 | Photolysis Cell[17]

Fig. (3) show the morphology of the synthesized BaO-NPs as determined by FE-SEM. A low-resolution image of prepared BaO-NPs with a flower-shaped cluster morphology is shown in, a high-resolution SEM picture, demonstrates the extremely crystalline growth of the produced nanomaterials. The SEM pictures also show that some NPs are arranged in structures resembling nanorods and nanosheets and are connected by accumulating on top of one another. By integrating EDS and SEM, the elemental composition analysis of produced NPs was evaluated. The chemical purity of the produced BaO-NPs was validated by EDS spectra. Where an analysis (EDX) as shown in fig.(4) shows that the nano-barium oxide is of high purity[19,20]. When an optically excited substance emits light spontaneously, it is called photoluminescence

(PL). In order to investigate various excitation types, determine the bandgap energy, find specific defects for radiative transitions, and determine the impurity levels in the nanomaterial sample, the excitation energy and intensity can be selected. The analysis method of photoluminescence spectroscopy is non-destructive fig. (5) depicts the photoluminescence spectra of BaO-NPs as it was measured at an excitation wavelength of 230 nm[21]. The spectrum displays two significant emission bands (Blue-violet and red). distinct peak are identified: a strong emission peak at 380nm.

The energy gap can be calculated according to the following equation:
For example (E v) = 1240 / λ..... [3)
Where Ev is the energy gap, and is the maximum wavelength.
And by the wavelength and according to the above equation, the energy gap of barium oxide is (3.26 ev).

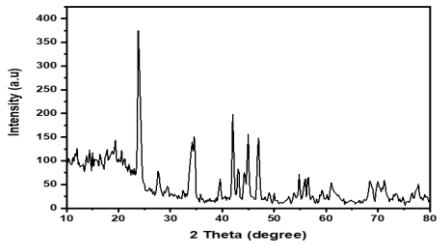

Figure 2 XRD image of barium oxide nanoparticles (BaO NPS)

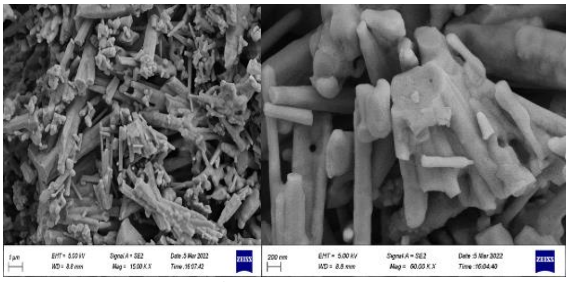

Fig. 3 | FE-SEM image of barium oxide nanoparticles (BaO NPS)

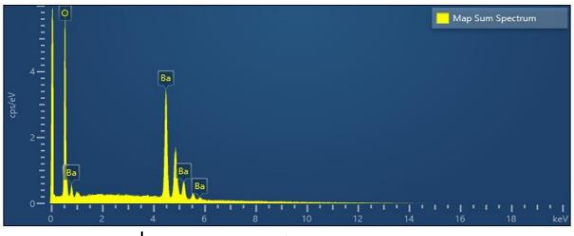

Fig. 4 | EDX images of Nanobarium Oxide (BaO NPS)

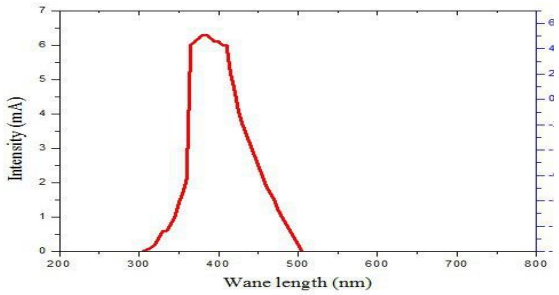

Fig. 5| Photoluminescence spectrum of BaO nanoparticles.

In previous studies, Barium nitrate $Ba(NO_3)_2$ and sodium bicarbonate NaHCO3 were used by Manauwar Ali Ansari et al. to prepare barium oxide nanoparticles using the co-precipitation method. the resultant of barium oxide nanoparticles from this method had a crystal size of 16–15 nm and energy gap 4.65ev [22].

In another study, The author Mohamed E. and his group prepared nano barium oxide (BaO NPS) using(BaCl2.2H2O), (NaOH) and (NH2)2CO with continuous stirring at a temperature of 50 and burning the precipitate at a temperature of 500C° , the NPs Size was to be 50[23].
The author E.Sundharam and his group prepared barium oxide by ultrasonication method using BaCl2.2H2O and NaOH temperature 400C° (4hr) Crystal size nanoparticles were 19.6 nm[24]
As the author Arvind k.Bhakta and his group prepared the nano-barium oxide using infrared irradiation and diazonium chemistry, and the crystal size was (3-18nm)[25].
In our method, The photolysis approach differs from other methods in that it is straightforward, quick, and inexpensive. In addition, it produces a lot of nanoparticles that are highly pure, have small crystal sizes, and are produced in vast amounts, as demonstrated by the current study.

3.2. *Adsorption isotherms*

To determine how the BaO NPS and cibacronblu interact, fit isotherm adsorption with the adsorption results. This project by Freundlich The correlation value R_2 demonstrates that Freundlich isotherm equations suit the adsorption *findings* as displayed in fig. (6) quite closely. The following equation represents the Freundlich adsorption's linearized form[26]

$$\text{Log}(Q_e) = \log(K_f) + 1/n \,.\, \log(C_e) \qquad (4)$$

Where *kf* and *n*, which are called the Freundlich constants, are the indicators of *adsorption* capacity and adsorption intensity, respectively[27]. The *kf* is gotten from the intercept and the *n* is obtained from the slope computed 1/n,

.

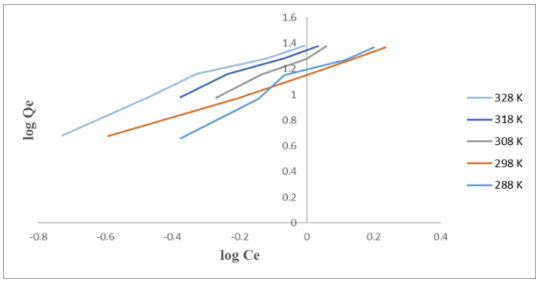

Fig. | 6 Freundlich straights for sepacron blue dye adsorption on BaO NPS at various temperatures

4-3 | Effect of contact Time

To achieve a balanced time, the time of contact was determined by mixing 0.01 g BaO NPS with 10 ml

of cibacron blue (25 ppm) in a sequence of tests. The mixture was shaken at 200 rpm under 298 K temperature. Fig. (7) shows the adsorption was extremely rapid at the beginning of 15–90 min. The fast adsorption came from a strong link between active BaO NPS and cibacron blue dye . Because of the occupancy on the BaO NPS surface, the adsorption rate of cibacron blue dye became constant after 90 mi[28].

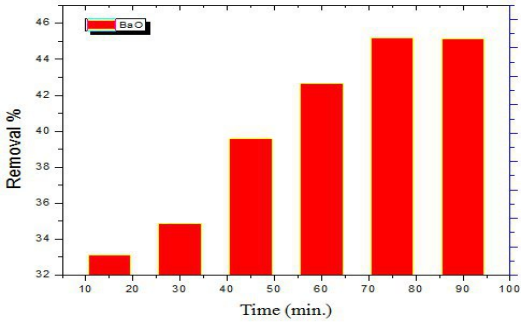

Fig. 7| Effect of time on adsorption of Siba Crohn F3GA blue dye at 25 C by BaO NPS

4-4 | *Effect of adsorbent mass*

After adding various amounts of BaO NPS, ranging from 0.01 to 0.2 g to 25 ppm of cibacron blue dye, the influence of the adsorbent mass was calculated. The concoction was 200 rpm shaken at 298 K temperature The quantity of Fig. (8) displays adsorbed as a function of mass. First of all the higher amount of the adsorption rate is due to active BaO NPS location. increased cibacron blue dye absorption was demonstrated by boosting the adsorbent mass29[30].

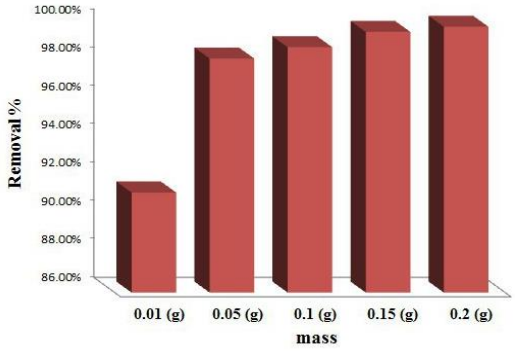

Fig. 8|The mass effect of BaO NPS on dye removal percentage

4-5 | Temperature effect and thermodynamic parameter calculation

At specific temperatures of 15°C, 25°C, 35°C, 45°C, and 55°C, the effect of temperature on cibacron blue dye adsorption on the surface of BaO NPS was investigated. With rising temperature, more cibacron blue dye adsorption solution was produced[31]. This indicates that the process was endothermic and that ΔH had a positive mean. Both the absorption and adsorption processes were demonstrated by this. The strong link that binds the adsorbate and the adsorbent was strengthened as a result of diffusion molecules being absorbed into the pores as the temperature climbed. The thermodynamic parameters (ΔH,ΔS,ΔG) give precise information on the associated adsorption-related intrinsic energy modifications, thus they must be evaluated properly. The following modifications were estimated in this study to predict the adsorption process using free energy ΔG32[33].

$$\text{Ln } K_e = -\Delta H/RT + \Delta S/R \quad (5)$$

$$K_e = Q_e/C_e \quad (6)$$

$$\Delta G = \Delta H - T\Delta S \quad (7)$$

where *Ke* is an equilibrium constant, *R* is a gas constant (8.314 J/mol K) and *T* is the temperature (K). From the slope . and interception of the plots of van't Hoff, ΔH and ΔS were identified as shown in Fig (10).

The corresponding ΔH from the slope was 9.697 kJ/mol, which indicated the process was endothermic. The ΔS from the intercept was 0.813 kJ/(mol K) that indicated the adsorbed molecules were still in constant motion on the surface, and they were attributable to absorption as well as adsorption. A higher temperature facilitated the adsorption of cibacron blue dye. The ΔG for adsorbing was determined to be 9.4303 kJ/mol at 298 K, which means spontaneous adsorption.

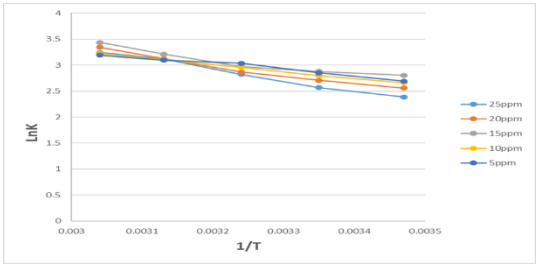

Fig. 10| (Van't Hoff) Scheme of adsorption of Siba Crohn blue dye by nanobarium oxide (BaO NPS) at different temperatures.

6 | Dynamics

To study adsorption, it is important to know the process kinetics to know the rate of pollutant removal from aqueous solutions. In order to determine the most suitable model for the adsorption of Cibacron F3GA blue on the surface of (NPS BaO), the evaluation was carried out using two orders, namely the false and the second order.

The adsorption of Cibacron F3GA blue dye on the surface of (BaO NPS) was applied to the pseudo-first-order by the equation[34]:

$$\text{Ln}(q_e-q_t)=\text{lnq}_e-K_1.t \quad \ldots\ldots\ldots (8)$$

where qt: the amount of dye adsorbed at each time (t min). qe: the amount of dye adsorbed at equilibrium (mg/g)). K1 : first-order constant (min^{-1}). Plotting the relationship between (lnqe-qt) versus time (t), which gives a linear relationship. as in Fig. (11).

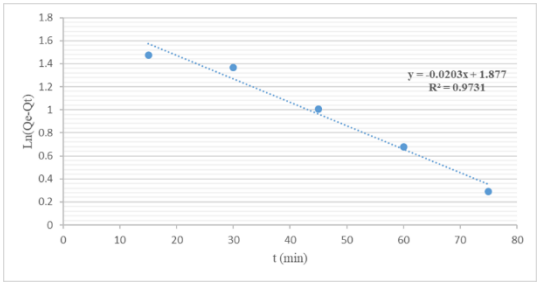

Fig. 11| False first order for adsorption of Siba Crohn blue pigment on (BaO NPS)at a temperature of 298 K

Where (R2) is (0.9731), K1 (Slope) is (-0.02031) in (min-1) units, and q_{exp} is equal to (1.876972) (intercept) in mg/g units.

The second order is given by the following relationship[35]:

t/qt = 1/K2 qe2 + (1/qe).t…….(9)

Where: qt the amount of dye adsorbed at any time in units (mg/g), qe the quantity of dye adsorbed at equilibrium in units ((mg/g, t)), adsorption time (min), K_2 is a pseudo-second-order equilibrium constant.

where t/q t is plotted against time (t) (min), qe can be calculated by slope, and K_2 can be calculated by (intercept) as in fig. (12) .

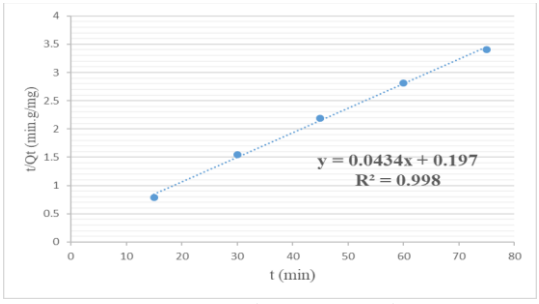

Fig. 12| False second order for adsorption of Siba Crohn blue pigment on the surface(BaO NPS) at a temperature of 298 K

where R_2 is(0.998), qe is(0.043352) in mg/g units, K_2 is 0.196996 in g/mg.min

Through the results, it is clear that the value of R_2 for the second order of dye adsorption by the BaO NPS is greater than R_1 for the first order, and this indicates that the adsorption proceeds according to the pseudo second order.

7 | Conclusion

quality of the rutile BaO NPS according to the XRD, SEM,PL characterizations. All the characterization techniques gave identical results to prove that the synthesized nano-BaO their average crystal size was calculated to be 14.6 nm. The nanoparticles proved to have excellent adsorption properties for removing cibacron blue dye from aqueous solutions. Both kinetic and dynamic studies were shown the efficiency of the BaO NPS adsorption. The results were fitted well with Freundlich isotherm model. The calculations of the thermodynamic parameters gave the adsorption values for ΔH, ΔS, and ΔG equal to 9.69 kJ/mol, 0.813 KJ/mol K, and 9.4303 kJ/mol, respectively. These results prove that the adsorption is an endothermic spontaneous process.

8. References

1. Nasrollahzadeh M, Issaabadi Z, Sajjadi M, Sajadi SM, Atarod M. *Types of Nanostructures*. Vol 28. 1st ed. Elsevier Ltd.; 2019.
2. Buzea C, Pacheco I. *Nanomaterials and Their Classification*. Vol 62.; 2017.
3. Yadav VK, Ali D, Khan SH, et al. Synthesis and characterization of amorphous iron oxide nanoparticles by the sonochemical method and their application for the remediation of heavy metals from wastewater. *Nanomaterials*. 2020;10(8):1-17.
4. Guo H, Xu Z, Jiang T, Zhao Y, Ma X, Wang S. The effect of incorporation Mg ions into the crystal lattice of CaO on the high temperature CO2capture. *J CO2 Util*. 2020;37(December 2019):335-345.
5. Zhou Y, Wang N, Qu X, et al. Arc-discharge synthesis of nitrogen-doped C embedded TiCN nanocubes with tunable dielectric/magnetic properties for electromagnetic absorbing applications. *Nanoscale*. 2019;11(42):19994-20005.
6. Maity JP, Hsu CM, Lin TJ, et al. Removal of fluoride from water through bacterial-surfactin mediated novel hydroxyapatite nanoparticle and its efficiency assessment: Adsorption isotherm, adsorption kinetic and adsorption Thermodynamics. *Environ Nanotechnology, Monit Manag*. 2018;9(November 2017):18-28.
7. Zhang H, Liu Q, Fang Y, et al. Boosting Zn-Ion Energy Storage Capability of Hierarchically Porous Carbon by Promoting Chemical Adsorption. *Adv Mater*. 2019;31(44):1-10. doi:10.1002/adma.201904948
8. Xia M, Chen Z, Li Y, et al. Removal of Hg(ii) in aqueous solutions through physical and chemical adsorption principles. *RSC Adv*. 2019;9(36):20941-20953.
9. Knoll S, Rösch T, Huhn C. Trends in sample preparation and separation methods for the analysis of very polar and ionic compounds in environmental water and biota samples. *Anal Bioanal Chem*. 2020;412(24):6149-6165.
10. AK B, J.Mascarenhas R, P M, J D, Mekhalif Z. Multi-wall Carbon Nanotubes Decorated with Barium Oxide Nanoparticles. *Synth Catal Open Access*. 2018;03(01).
11. Naz F, Saeed K. Synthesis of barium oxide nanoparticles and its novel application as a catalyst for the photodegradation of malachite green dye. *Appl Water Sci*. 2022;12(6):1-11.
12. Routoula E, Patwardhan S V. Degradation of Anthraquinone Dyes from Effluents: A Review Focusing on Enzymatic Dye Degradation with

Industrial Potential. *Environ Sci Technol*. 2020;54(2):647-664.
13. Bouhadjra K, Lemlikchi W, Ferhati A, Mignard S. Enhancing removal efficiency of anionic dye (Cibacron blue) using waste potato peels powder. *Sci Rep*. 2021;11(1):1-10.
14. Fröse A, Schmidtke K, Sukmann T, Juhász Junger I, Ehrmann A. Application of natural dyes on diverse textile materials. *Optik (Stuttg)*. 2019;181:215-219.
15. Nayak A, Bhushan B. Hydroxyapatite as an advanced adsorbent for removal of heavy metal ions from water: Focus on its applications and limitations. *Mater Today Proc*. 2021;46(xxxx):11029-11034.
16. Kamil AF, Abdullah HI, Rheima AM. Fabrication of Dye-sensitized Solar Cells and Synthesis of CuNiO2 Nanostructures Using a Photo-irradiation Technique. *J Nanostructures*. 2022;12(1):144-159.
17. Hussein SKA, Rheima AM, Al Kazaz FF, Mohammed SH, Al-Khateeb IKI. New synthesis of quantum dots copper sulfide using the UV-irradiation technique. *Chalcogenide Lett*. 2022;19(5):363-370.
18. Khalaf RL, Almousawi IM, Rheima AM. Uv-Irradiation synthesized Co3ZnFe2O8 Nanoparticles for Corrosion Protection of Carbon Steel in Seawater. Egyptian Journal of Chemistry. 2022 Jul 18.
19. Sherlala AIA, Raman AAA, Bello MM, Buthiyappan A. Adsorption of arsenic using chitosan magnetic graphene oxide nanocomposite. *J Environ Manage*. 2019;246(January):547-556.
20. Mohammed SH, Rheima A, Al-jaafari F, Al-Marjani MF. Green-synthesis of Platinum Nanoparticles using Olive Leaves Extracts and its Effect on Aspartate Aminotransferase Activity. Egyptian Journal of Chemistry. 2022 Apr 1;65(4):1-2.
21. Ansari MA, Jahan N. Structural and Optical Properties of BaO Nanoparticles Synthesized by Facile Co-precipitation Method. *Mater Highlights*. 2021;2(1-2):23.
22 Ansari MA, Jahan N. Structural and Optical Properties of BaO Nanoparticles Synthesized by Facile Co-precipitation Method. *Mater Highlights*. 2021;2(1-2):23.
23. Mahmoud ME, Khalifa MA, El-Sharkawy RM, Youssef MR. Effects of Al2O3 and BaO nano-additives on mechanical characteristics of high-density polyethylene. *Mater Chem Phys*. 2021;262(January):124251.
24 Sundharam E, Jeevaraj AKS, Chinnusamy C. Effect of ultrasonication on the synthesis of barium oxide nanoparticles. *J Bionanoscience*. 2017;11(4):310-314.
25 Bhakta, Arvind K., et al. "Methylene Blue Dye Removal Through Adsorption Onto Amorphous BaO Nanoparticles Decorated MWCNTs." *Materials Research and Applications*. Springer, Singapore, 2021. 231-240.
26. Litefti K, Freire MS, Stitou M, González-Álvarez J. Adsorption of an anionic dye (Congo red) from aqueous solutions by pine bark. *Sci Rep*. 2019;9(1):1-11.
27. Maleki A, Mohammad M, Emdadi Z, Asim N, Azizi M, Safaei J. Adsorbent materials based on a geopolymer paste for dye removal from aqueous solutions. *Arab J Chem*. 2020;13(1):3017-3025.
28. Piri F, Mollahosseini A, Khadir A, Milani Hosseini M. Enhanced adsorption of dyes on microwave-assisted synthesized magnetic zeolite-hydroxyapatite nanocomposite. *J Environ Chem Eng*. 2019;7(5):103338.
29. Gould NS, Li S, Cho HJ, et al. Understanding solvent effects on adsorption and protonation in porous catalysts. *Nat Commun*. 2020;11(1):1-13.
30. Sowmyashree AS, Somya A, Kumar CBP, Rao S. Novel nano corrosion inhibitor, integrated zinc titanate nano particles: Synthesis, characterization, thermodynamic and electrochemical studies. *Surfaces and Interfaces*. 2021;22:100812.
31. Kumar A, Kumar M, Kumar R, Singh R, Prasad B, Kumar D. Numerical model for the chemical adsorption of oxygen and reducing gas molecules in presence of humidity on the surface of semiconductor metal oxide for gas sensors applications. *Mater Sci Semicond Process*. 2019;90(June 2018):236-244
32. Hussain DH, Rheima AM, Jaber SH. Cadmium ions pollution treatments in aqueous solution using electrochemically synthesized gamma aluminum oxide nanoparticles with DFT study. Egyptian Journal of Chemistry. 2020 Feb 1;63(2):417-24.
33. Mahmood RS. The uptake of Eriochrome Black T dye from Wastewater utilizing synthetized Cadmium Sulfide Nanoparticles. Egyptian Journal of Chemistry. 2022 Jun 1;65(6):1-2.
34 Kamil AF, Abdullah HI, Mohammed SH. Cibacron red dye removal in aqueous solution using synthesized CuNiFe2O5 Nanocomposite: thermodynamic and kinetic studies. Egyptian Journal of Chemistry. 2021 Nov 1;64(11):5-6.
35 Mohammed MA, Rheima AM, Jaber SH, Hameed SA. The removal of zinc ions from their aqueous solutions by Cr2O3 nanoparticles synthesized via the UV-irradiation method. Egyptian Journal of Chemistry. 2020 Feb 1;63(2):425-31.